Effect of cold collisions on spin coherence and resonance shifts in a magnetically trapped ultracold gas

D. M. Harber, H. J. Lewandowski, J. M. McGuirk,* and E. A. Cornell*

JILA, National Institute of Standards and Technology and Department of Physics, University of Colorado, Boulder, Colorado 80309-0440

We have performed precision microwave spectroscopy on ultracold ^{87}Rb confined in a magnetic trap, both above and below the Bose-condensation transition. The cold collision frequency shifts for both normal and condensed clouds were measured, which allowed the intrastate and interstate density correlations (characterized by sometimes controversial "factors of 2") to be determined. Additionally, temporal coherence of the normal cloud was studied, and the importance of mean-field and velocity-changing collisions in preserving coherence is discussed.

With the advent of modern cooling and trapping techniques, the cold collision regime has become readily accessible. In the cold collision regime quantum statistical effects due to particle indistinguishability dominate scattering processes. The symmetrization requirement for identical particles in an ultracold Bose gas enhances the probability of finding two particles nearby causing density fluctuations. At lower temperatures the statistical nature of the Bose gas causes the phenomena of Bose-Einstein condensation, where all atoms in the condensate share the same wave function, suppressing the density fluctuations found in a noncondensed sample.

Suppression of second-order density fluctuations in a condensate has been measured through analysis of the expansion energy of condensates [1,2]. In a separate experiment, the suppression of third-order density fluctuations was probed by comparing the three-body loss rate of a condensate to that of a normal cloud [3]. The effect of cold collisions has also been measured as a density-dependent energy shift in atomic fountain clocks [4–6]. These shifts are quite small ($\sim 0.1–10$ mHz) due to the low densities at which the clocks operate, but are measurable because of their high precision. The uncertainty associated with these collisional shifts can be problematic; in fact the next generation of atomic fountain clocks are based on ^{87}Rb rather than ^{133}Cs because the collisional shift of ^{87}Rb is ~ 30 times smaller. In recent ultracold hydrogen experiments the cold collision shift provided the signature of Bose condensation; below the transition a large frequency shift of the $1S$-$2S$ transition was seen, reflecting the high density of the condensate [7].

In this paper we report precision microwave spectroscopy performed on ultracold and condensed ^{87}Rb atoms confined in a magnetic trap. Due to the high densities achievable in a magnetic trap, the collisional energy shifts were 10^5 times greater than those in ^{87}Rb atomic clocks, allowing a high-precision measurement of the shifts of the magnetically trappable states to be made with relative ease. The collisional

shifts for both a normal and condensed sample were measured, providing a useful probe of the quantum statistics of the system. Additionally, magnetic confinement permits long interrogation times, allowing us to characterize temporal coherence of the normal cloud under various experimental conditions. Comparison of measured coherence times with a collisionless numerical simulation suggests that collisions preserve coherence in normal clouds.

Precision spectroscopy of trapped samples is difficult because atom trapping relies on spatial inhomogeneity of the atomic energy levels. Spatial inhomogeneity of the energy levels broadens the transition frequency, thus limiting the precision attainable through spectroscopy. In other work, this difficulty has been avoided by confining atoms in a blue-detuned optical dipole trap, where atoms spend little time interacting with the trapping fields [8]. In this work spatial inhomogeneity of the transition frequency was minimized through the use of a pair of energy levels which experience the same trapping potential. At a magnetic field of ~ 3.23 G, the $|1\rangle \equiv |F=1, m_f=-1\rangle$ and $|2\rangle \equiv |F=2, m_f=1\rangle$ hyperfine levels of the $5S_{1/2}$ ground state of ^{87}Rb experience the same first-order Zeeman shift. For a normal cloud at 500 nK, each energy level is Zeeman shifted by ~ 10 kHz across the extent of the cloud; however, at 3.23 G the *differential* shift of the two levels across the cloud is ~ 1 Hz. Compared to the differential Zeeman shift, the energy shift due to cold collisions has then a relatively large effect at high densities, making measurements of collisional shifts in this system possible. The small inhomogeneity allows for long coherence times, ~ 2 s and longer for low-density clouds, making this system attractive for precision measurements as well as for the study of condensate coherence in the presence of a thermal cloud.

The experimental setup has been previously described [9] and will be briefly summarized here. Approximately 10^9 ^{87}Rb atoms are loaded into a vapor cell magneto-optical trap (MOT). The atoms are then optically pumped into the $|F=1\rangle$ state by turning off the repump beam while MOT beams remain on. Then the trapping beams are turned off and the MOT coils are ramped to a high current forming a 250 G/cm gradient to trap $|1,-1\rangle$ atoms in the quadrupole field of the coils. The quadrupole coils are mounted on a linear servo-motor controlled track which then moves the coils 44

---

*Also at Quantum Physics Division, National Institute of Standards and Technology.

cm, from the MOT region to a Ioffe-Pritchard trap in the ultrahigh vacuum region of the system. The Ioffe-Pritchard trap consists of two permanent magnets which provide a 450 G/cm radial gradient. Two pairs of electromagnetic coils, a pinch and a bias, provide confinement in the axial direction, which is aligned perpendicular with respect to gravity. At a typical bias field of 3.23 G, atoms in the $|1,-1\rangle$ state experience $\{230,230,7\}$ Hz trap frequencies. The sample is further cooled by rf evaporation, and condensates of up to 10^6 atoms can be formed. Imaging is performed by the use of adiabatic rapid passage to transfer atoms from the $|1,-1\rangle$ state to the $|2,-2\rangle$ state. Antitrapped $|2,-2\rangle$ atoms rapidly expand for 2–5 ms and then are imaged through absorption by a 20 μs pulse of $5S_{1/2}|2,-2\rangle \rightarrow 5P_{3/2}|3,-3\rangle$ light.

A two-photon microwave-rf transition is used to transfer atoms between the $|1\rangle$ and $|2\rangle$ states. A detuning of 0.7 MHz from the $|2,0\rangle$ intermediate state provides a two-photon Rabi frequency of $\sim$2.5 kHz. Ramsey spectroscopy of the $|1\rangle \rightarrow |2\rangle$ transition is performed by measuring the total number of atoms remaining in state $|1\rangle$ after a pair of $\pi/2$ pulses separated by a variable time delay is applied [10]. The frequency of the resulting Ramsey fringes is the difference between the transition frequency ν_{12} and the two-photon drive frequency. In previous work we measured local variations of ν_{12} by detecting the number of atoms remaining in state $|1\rangle$ at specific spatial locations along the axis of the normal cloud [9]. By analyzing the spatio-temporal variations of ν_{12}, combined with the measured evolution of the $|1\rangle$ state after a single $\pi/2$ pulse, we were able to spatially resolve the evolution of spin waves [11]. In this work, in order to perform measurements of ν_{12} insensitive to spin waves, one of the following two techniques was used. With one technique the entire cloud, rather than specific spatial locations, was monitored to average out the effects of spin waves. Alternatively, Ramsey spectroscopy was restricted to interrogation times short compared to the spin-wave frequency [12].

One effect which shifts the transition frequency ν_{12} is the differential Zeeman shift. The Breit-Rabi formula predicts a minimum in ν_{12} at $B_0 = 3.228\,917(3)$ G, thus the differential Zeeman shift between the $|1\rangle$ and $|2\rangle$ energy levels is a first-order magnetic field independent at $B = B_0$. The differential Zeeman shift about B_0 can be approximated as $\nu_{12} = \nu_{min} + \beta(B - B_0)^2$ [13]. Measuring ν_{12} for different magnetic fields allows us to calibrate our magnetic field from the expected dependence, see Fig. 1. By working in the vicinity of $B = B_0$ we greatly reduce spatial inhomogeneity of ν_{12} and also become first-order insensitive to temporal magnetic-field fluctuations.

A second effect that shifts ν_{12} arises from atom-atom interactions. In the *s*-wave regime, where the thermal de Broglie wavelength of the atoms is greater than their scattering length, atoms experience an energy shift equal to $\alpha(4\pi\hbar^2/m)an$, where α is the two-particle correlation at zero separation, n is the atom number density, a is the scattering length, and m is the atom mass. Therefore, for a two-component sample the expected energy shift of each state is

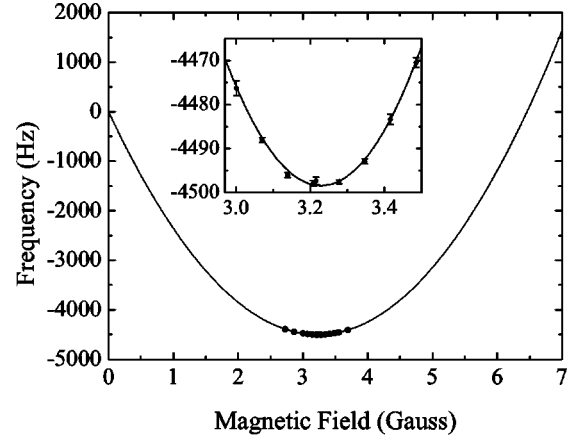$$\delta\mu_1 = \frac{4\pi\hbar^2}{m}(\alpha_{11}a_{11}n_1 + \alpha_{12}a_{12}n_2), \qquad (1)$$

FIG. 1. Differential Zeeman shift at low magnetic fields for the $|1\rangle \rightarrow |2\rangle(|F=1,m_f=-1\rangle \rightarrow |F=2,m_f=1\rangle)$ transition. The solid line is the predicted splitting from the Breit-Rabi formula. The inset plot expands the bias field region where most studies are performed.

$$\delta\mu_2 = \frac{4\pi\hbar^2}{m}(\alpha_{12}a_{12}n_1 + \alpha_{22}a_{22}n_2), \qquad (2)$$

where n_1 and n_2 are the $|1\rangle$ and $|2\rangle$ state densities and

$$\alpha_{ij} = \frac{\langle\Psi_i^\dagger\Psi_j^\dagger\Psi_i\Psi_j\rangle}{\langle\Psi_i^\dagger\Psi_i\rangle\langle\Psi_j^\dagger\Psi_j\rangle}. \qquad (3)$$

The shift of the transition frequency in Hz can then be written as

$$\Delta\nu_{12} = \frac{2\hbar}{m}(\alpha_{12}a_{12}n_1 + \alpha_{22}a_{22}n_2 - \alpha_{11}a_{11}n_1 - \alpha_{12}a_{12}n_2)$$

$$= \frac{\hbar}{m}n[\alpha_{22}a_{22} - \alpha_{11}a_{11} + (2\alpha_{12}a_{12} - \alpha_{11}a_{11}$$

$$- \alpha_{22}a_{22})f], \qquad (4)$$

where $f = (n_1 - n_2)/n$ and $n = n_1 + n_2$.

For noncondensed, indistinguishable bosons, $\alpha = 2$ due to exchange symmetry, therefore $\alpha_{11}^{nc} = \alpha_{22}^{nc} = 2$ in a cold normal cloud (where the superscript c or nc refers to condensed of noncondensed atoms, respectively). Distinguishable particles do not maintain exchange symmetry, making $\alpha_{12}^{nc} = 1$ for an incoherent two-component mixture. However if a two-component sample is prepared by coherently transferring atoms from a single component, such as in Ramsey spectroscopy, then the excitation process maintains exchange symmetry, and we might expect $\alpha_{12}^{nc} = 2$ [14]. In this scenario the collisional shift should be calculated using $\alpha_{11}^{nc} = \alpha_{22}^{nc} = \alpha_{12}^{nc} = 2$, leading to a predicted frequency shift of

$$\Delta\nu_{12} = \frac{2\hbar}{m}n[a_{22} - a_{11} + (2a_{12} - a_{11} - a_{22})f]. \qquad (5)$$

This result can also be obtained by solving the transport equation [15,16]. From spectroscopic studies [17] the three ^{87}Rb scattering lengths of interest have been determined to
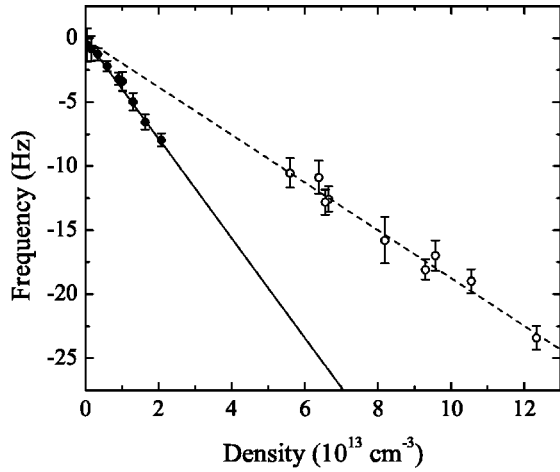
FIG. 2. Measurement of the cold collision shift. Solid and open circles represent measurements of the normal cloud and condensate, respectively. The solid line is a fit to the normal cloud data $\Delta \nu_{12} = 0.1(0.4) - 3.9(0.3)10^{-13}n$; the dashed line is a fit to the condensate data $\Delta \nu_{12} = -0.1(1.4) - 1.9(0.2)10^{-13}n$ where $\Delta \nu_{12}$ is in Hz and n is in cm^{-3}.

be $a_{22} = 95.47a_0$, $a_{12} = 98.09a_0$, and $a_{11} = 100.44a_0$, where a_0 is the Bohr radius. The frequency shift can then be written as

$$\Delta \nu_{12} = \frac{2\hbar}{m} a_0 n (-4.97 + 0.27f). \qquad (6)$$

If on the other hand the $|1\rangle$ and $|2\rangle$ states do *not* maintain exchange symmetry, such that $\alpha_{12}^{nc} = 1$, then the frequency shift would instead be

$$\Delta \nu_{12} = \frac{2\hbar}{m} a_0 n (-4.97 - 97.82f). \qquad (7)$$

These two models are clearly distinguished by the dependence of ν_{12} on f.

When we perform Ramsey spectroscopy with a pair of $\pi/2$ pulses, the populations of the $|1\rangle$ and $|2\rangle$ states are equal, and thus $f = 0$ during the interrogation time. From Eq. (4) it is apparent that with $f = 0$ the collisional shift is sensitive only to α_{ii}^{nc} and a_{ii} terms. For these measurements the bias field was set to B_0, and the transition frequency was measured for a range of densities. To adjust density of the sample, the number of atoms in the initial MOT load was varied. All normal cloud data were taken at the same temperature of 480 nK, and all condensate data were taken with high condensate fractions in order to minimize effects due to the normal cloud. The density for the normal cloud was found by fitting Gaussian profiles to absorption images of the clouds and extracting the number, temperature, and density. To measure condensate density, Thomas-Fermi profiles were fit to absorption images of the condensates and the total number N_0 in the condensates and the Thomas-Fermi radius along the long axis Z were extracted.

The results of this measurement are shown in Fig. 2. Comparing the collisional shift measured for the normal

cloud to that measured for a condensate gives $\alpha_{ii}^{nc}/\alpha_{ii}^c = 2.1(2)$. If instead we *assume* $\alpha_{ii}^{nc} = 2$ and $\alpha_{ii}^c = 1$, then the data for both the condensate and normal cloud can be used to obtain a value for the difference in scattering lengths of $a_{22} - a_{11} = -4.92(28)a_0$, in agreement with values determined from molecular spectroscopy [17].

Many systematics can plague density measurements made through absorption imaging. In order to test independently our density calibration for both the normal and condensed samples, each of which can suffer from different errors, we used the Bose-condensation phenomenon. The density of normal clouds was tested through measurement of the critical temperature, and condensate density was tested with the Thomas-Fermi approximation. Assuming that disagreements are only due to the errors in the estimation of atom number, the worst-case scenario, leads us to reduce normal cloud density by 11(4)% and increase condensate density by 11(3)%. Adjusting the cold collision shifts accordingly would yield a worst-case corrected value of $\alpha_{ii}^{nc}/\alpha_{ii}^c = 1.7(2)$ [18]. The adjusted normal and condensate density shifts can be combined as above to give a value for the difference in scattering lengths of $a_{22} - a_{11} = -4.85(31)a_0$; not significantly different from our unadjusted measurement.

The remaining significant systematic is atom loss due to $|2\rangle$-$|2\rangle$ collisional dipolar relaxation. In order to minimize effects of this loss, interrogation times were kept as short as possible. Nevertheless, for the highest-density condensate measurements the $|2\rangle$-$|2\rangle$ loss causes the total density to drop by 3% in 20 ms, the maximum interrogation time. For all other densities the loss was no larger than this, and in most cases much smaller. Finally, the $|1\rangle$ and $|2\rangle$ states begin undergoing spatial separation in the condensate after the first $\pi/2$ pulse [19]; however, the time scale for the separation is much longer than our 20 ms interrogation time.

Exchange symmetry between the $|1\rangle$ and $|2\rangle$ states can be tested by working at a fixed density and varying the relative $|1\rangle$ to $|2\rangle$ population by varying the length of the first Ramsey pulse [20]. In this case the first term in Eq. (4) will be constant and the measurement will test α_{12}^{nc} and a_{12} as well as the α_{ii}^{nc} and a_{ii} terms [see Eqs. (6) and (7)]. To minimize systematics the interrogation times were kept short, making precise frequency determination difficult. Nevertheless, our measurement (Fig. 3) indicates $\alpha_{12}^{nc}/\alpha_{11,22}^{nc} = 1.01(2)$, where we have used the spectroscopically determined scattering lengths. This clearly indicates that exchange symmetry is maintained between the $|1\rangle$ and $|2\rangle$ states. A similar measurement was made on the $|F = 1, m_f = 0\rangle \rightarrow |F = 2, m_f = 0\rangle$ transition by Fertig and Gibble [5].

As a thought experiment, imagine distinct thermal populations of $|1\rangle$ and $|2\rangle$ atoms, separately prepared, then mixed together, with the energy of interaction (proportional to α_{12}^{nc}) measured, for instance, calorimetrically. Surely in this case the density fluctuations in state $|1\rangle$ and in state $|2\rangle$ would be uncorrelated, and α_{12}^{nc} would be determined to be 1, not 2. We lack the experimental sensitivity to make such a calorimetric measurement, and our Ramsey-fringe method of measuring energy differences obviously would not work for incoherent mixtures. We speculated, however, that if $\alpha_{12}^{nc} = 2$
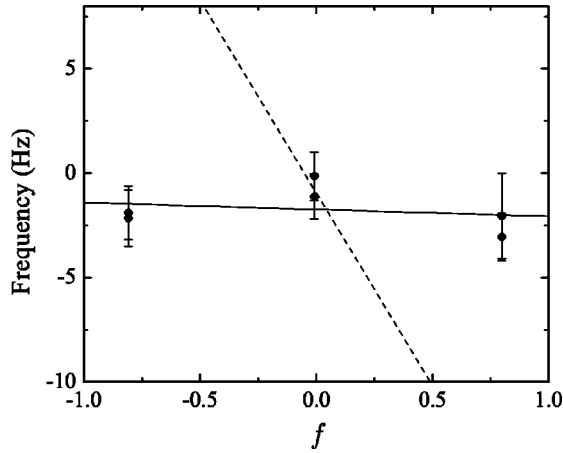
FIG. 3. Testing the exchange symmetry between the $|1\rangle$ and $|2\rangle$ states. The transition frequency is measured as $f = (n_1 - n_2)/n$, is varied for a normal cloud at a fixed peak density of 7×10^{12} cm^{-3} and temperature of 510 nK. The solid line is the fit, which yields $\alpha_{12}^{nc}/\alpha_{11,22}^{nc} = 1.01(2)$, which is to say, interstate and intrastate density correlations are quite accurately the same. The dotted line indicates the expected slope for $\alpha_{12}^{nc}/\alpha_{11,22}^{nc} = 1/2$.

for coherent superpositions, and if $\alpha_{12}^{nc} = 1$ for incoherent mixtures, then for partially decohered samples, α_{12}^{nc} would take on some intermediate value. So by performing a measurement similar to that in Fig. 3 we might expect to see a more negative slope for a partially decohered sample; alternatively, a frequency chirp in the Ramsey fringes may be seen as the sample decoheres.

We probed the time evolution of α_{12}^{nc} in a way similar to Fig. 3; however, rather than varying f we set $f \simeq 0.8$ then measured ν_{12} with long interrogation times, looking for a frequency chirp as the fringe contrast decreased. This method has the advantage that there is a relatively small $|2\rangle$ state population, so effects arising from $|2\rangle$ loss are minimized. Seven data sets were taken for this measurement; an example is shown in Fig. 4. By allowing a linear frequency
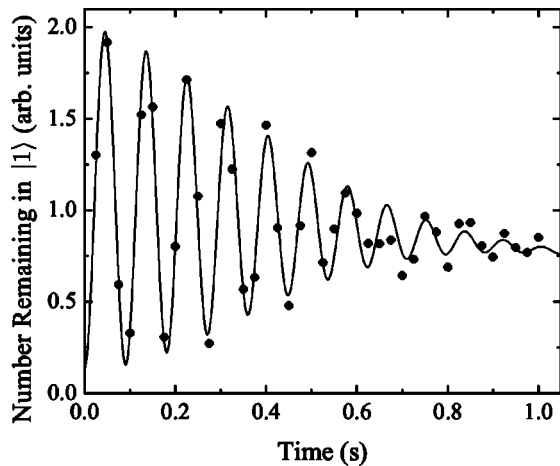

FIG. 4. A data set of Ramsey fringes probing for frequency shifts as a function of coherence. For this measurement normal clouds at a temperature of 480 nK and a peak density of 3.2 $\times 10^{13}$ cm^{-3} were used.

chirp in the fit of the Ramsey fringes, the frequency shift can be constrained to $-0.2(3)$ Hz by the time the fringe contrast has reduced to $1/e$ [21]. However, if we hypothesize that α_{12}^{nc} goes from 2 to 1 linearly as fringe contrast goes from 100% to 0% we would expect a frequency shift of $-20(2)$ Hz as the fringe decayed, while the experimental limit is 40 times smaller. Clearly this is appealing but unrigorous model is far too naive.

Ramsey spectroscopy not only allows us to probe the energy difference between the two states, but also permits the measurement of the coherence between the two states. Coherence measurements were performed using the same time domain method used to measure ν_{12}; however, interrogation times were extended until the Ramsey fringe contrast was lost. The resulting data were fit to a $e^{-(t/\tau)^2}$ decay, where τ is the coherence time. Additionally, fitting allowed for both a loss in total atom number and a linear frequency chirp of ν_{12}. To ensure that the $1/e$ atom loss times were much longer than the coherence times, fractional transfers ($f \simeq 0.8$) to the $|2\rangle$ state were used for the high-density data points. The results of coherence measurements for different magnetic fields and at three different densities are shown in Fig. 5.

We expect that the primary source of decoherence is inhomogeneity in ν_{12} across the cloud, to which both the differential Zeeman and collisional shifts contribute. The collisional shift scales directly with density, and thus provides a Gaussian-shaped ν_{12} profile across the cloud [9]. Inhomogeneity arising from the differential Zeeman effect depends on the bias field. The magnitude of the magnetic field near the bottom of the trap can be written as $B(z) = (B''/2) z^2 + B_{bias}$, thus the inhomogeneity due to the Zeeman shift is $\nu_{12} \propto (B''^2/4) z^4 + (B_{bias} - B_0) B'' z^2$. By setting $B_{bias}(>, <, =) B_0$ the curvature of ν_{12} can be adjusted to be positive, negative, or nearly zero, respectively. This allows inhomogeneity due to the collisional shift to be roughly canceled by an opposing Zeeman inhomogeneity [9]. This cancelation can be seen in Fig. 5; as the density is increased from (a) to (c), the inhomogeneity induced by the collisional shift increases, so that a larger opposing Zeeman inhomogeneity is necessary for cancellation. Therefore, the bias field for peak coherence time decreases as cloud density increases.

In an attempt to compare the measured decoherence times to the known spatial inhomogeneity of the transition frequency, we performed the following numerical simulation: consistent with a Maxwell-Boltzman distribution, we randomly assign initial positions and velocities to 10 000 simulated atoms. Ignoring the effects of collisions, we calculate the three-dimensional trajectory of each atom for several simulated seconds, keeping track of the time integral of ν_{12} along the trajectory. At each point in time, we calculate the spatially integrated transverse magnetization and, as inhomogeneities cause this magnetization to wash out, find the time it takes the integrated transverse magnetization to reduce to $1/e$ of its original value [22]. This model should correctly account for the effect of motional averaging except that all collisional effects are explicitly excluded. The resulting modeled damping times are plotted as a solid line along with the
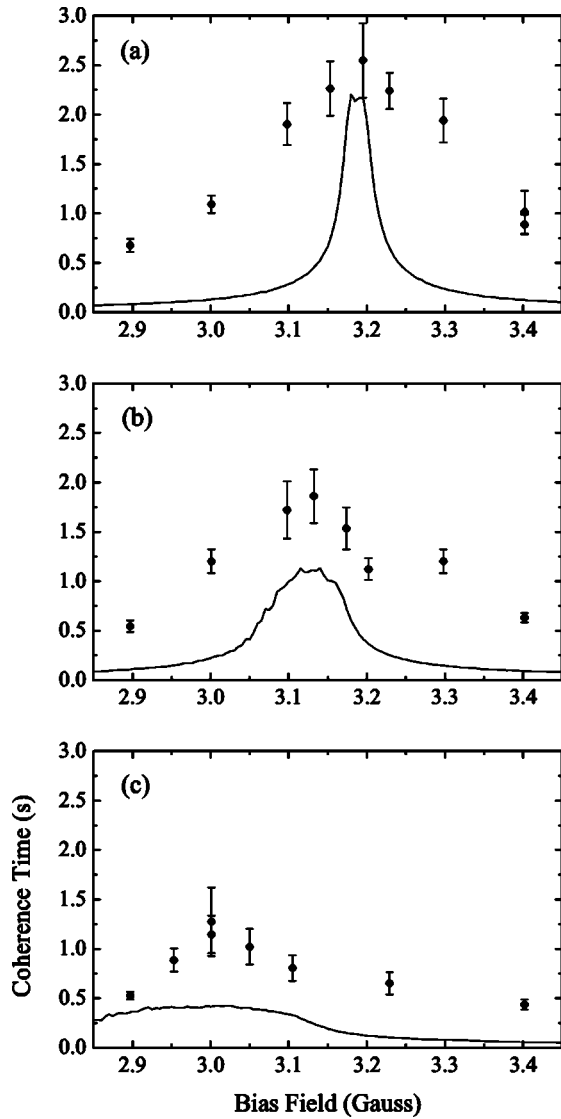
FIG. 5. Coherence times in a normal cloud. The temperature was ~480 nK and the normal cloud peak density for each plot is (a) 4×10^{12} cm^{-3}; (b) 1.3×10^{13} cm^{-3}; (c) 3.2×10^{13} cm^{-3}. The solid line in each plot corresponds to the $1/e$ times obtained from a numerical simulation (see text). The noise in the simulation data is due to the finite number of particles used and the random initialization.

experimentally measured damping times in Fig. 5. While the model does a reasonable job predicting the value of the bias field for which the coherence time peaks, it consistently underestimates (in some cases by a factor of 8) the actual value of the coherence time. Our model neglects both velocity-changing collisions and the exchange-type collisions that lead to spin waves; it appears that these effects contribute significantly to preserving coherence across the trapped atom cloud.

The extreme aspect ratio of our trapped cloud complicates a proper quantitative analysis of the effects of collisions on coherence. Along the axial direction, our previous work has shown that the effects of spin waves are to keep local magnetization across the cloud from straying too far from its spatially averaged value [see in particular Fig. 2(a) of Ref. [11]]. In the radial directions, the motional oscillation frequency exceeds the mean-field exchange frequency in the cloud, and thus the effects of spin waves are probably not relevant. On the other hand, velocity-changing collisions are likely important—in their absence, atoms with small transverse energies would stay near the axis of the trap, while atoms with large transverse energies would preferentially sample the larger magnetic fields and lower densities further from the axis. Velocity-changing collisions which re-randomize the transverse trajectories of these different classes of atoms (before they have a time to accumulate a radian or more of relative phase difference) will serve to extend the coherence time of the sample. In the highest-density data set presented [Fig. 5(c)] the mean elastic collision rate was 74 Hz, which should be compared with the measured coherence times of around 0.5 to 1.2 seconds.

It is interesting to consider the usefulness of magnetically trapped atoms for precision metrology. Peak coherence times of ≈ 2.5 s were realized with cold, low-density samples. An interrogation time of 2.5 s provides a 0.2 Hz linewidth, which naturally leads one to consider using such a system for precision measurements. By working at $B_{bias} = B_0$, coherence times are slightly reduced. However, perturbations of ν_{12} due to magnetic-field fluctuations become very small, on the order of 4 mHz for current typical experimental conditions. With careful design of the confinement coils, the current supply, and magnetic shielding of external fields, it should be possible to suppress fluctuations of the bias field below 1 mG, reducing Zeeman-induced frequency shifts to below 0.1 mHz. Perturbations of ν_{12} due to the cold collision shift are more significant; shot-to-shot density fluctuations will introduce frequency noise, so it is advantageous to work with the minimum possible density. However, as the atom number is reduced the maximum signal-to-noise ratio will decrease due to shot noise [23], therefore the optimum strategy is to work with an atom number such that the frequency uncertainty due to shot noise is on the order of the uncertainty due to density fluctuations.

For example, a normal cloud of 400 nK and a peak density 1.5×10^{12} cm^{-3} has 6×10^4 atoms. The shot-noise-limited signal-to-noise ratio is then 245:1. With an interrogation time of 1 s the single-shot statistical uncertainty is then 0.65 mHz; including the effects of decoherence and atom loss will increase this to ≈ 0.9 mHz. Assuming that the shot-to-shot number fluctuations are also shot-noise limited, then statistical uncertainty from the density shift is 0.84 mHz. Combining these gives a total single-shot uncertainty of 1.24 mHz; with our current 30 s evaporation time, the duty-cycle is such that an absolute precision of 6.8 mHz/$\sqrt{\text{Hz}}$ can be realized. This corresponds to a relative precision of $1 \times 10^{-12} / \sqrt{\text{Hz}}$, which in terms of measurement precision does not reach the level of atomic fountain clocks. This system, however, has the advantage that small energy shifts can be measured in a compact, stationary spatial position; a 400 nK cloud occupies approximately only a $1040 \times 32 \times 32$ μm region of space. It is certainly feasible to perform

spectroscopy at this level within 100 μm of a surface, which might allow the measurement of short-range atom-surface interactions.

In future work we plan on measuring coherence times in finite temperature condensates to study the role of the normal cloud in decoherence. We anticipate that this system will be quite rich due to the existence of spin waves in the normal component, phase separation in the condensate, and the interaction between the two. The complexity of this interaction may partially account for the anomalous density shift of the condensate seen in the hydrogen experiments [7,14].

We have demonstrated precise spectroscopy in an ultra-cold magnetically trapped gas. This permitted measurement of the cold collision shift in both a condensate and a normal cloud, allowing a probe of the quantum statistics of the system. Working at low densities minimizes the effect of the collisional shift, allowing long coherence times and precise determination of ν_{12}; however, the measurement of any quantity not related to atom-atom interactions will at some level be limited by this shift. An intriguing alternative would be to instead use a fermionic atom, which should have no collisional shift, and thus density induced frequency noise will not be an issue. On the other hand, the lack of collisions may also lead to more rapid decoherence: collisions appear to preserve our bosonic system from the decohering effects of spatial inhomogeneity.

[1] M.J. Holland, D.S. Jin, M.L. Chiofalo, and J. Cooper, Phys. Rev. Lett. **78**, 3801 (1997).

[2] W. Ketterle and H.-J. Miesner, Phys. Rev. A **56**, 3291 (1997).

[3] E.A. Burt, R.W. Ghrist, C.J. Myatt, M.J. Holland, E.A. Cornell, and C.E. Wieman, Phys. Rev. Lett. **79**, 337 (1997).

[4] K. Gibble and S. Chu, Phys. Rev. Lett. **70**, 1771 (1993).

[5] C. Fertig and K. Gibble, Phys. Rev. Lett. **85**, 1622 (2000).

[6] Y. Sortais, S. Bize, C. Nicolas, A. Clairon, C. Salomon, and C. Williams, Phys. Rev. Lett. **85**, 3117 (2000).

[7] T.C. Killian, D.G. Fried, L. Willmann, D. Landhuis, S.C. Moss, T.J. Greytak, and D. Kleppner, Phys. Rev. Lett. **81**, 3807 (1998); D.G. Fried, T.C. Killian, L. Willmann, D. Landhuis, S.C. Moss, D. Kleppner, and T.J. Greytak, *ibid.* **81**, 3811 (1998).

[8] N. Davidson, H.J. Lee, C.S. Adams, M. Kasevich, and S. Chu, Phys. Rev. Lett. **74**, 1311 (1995).

[9] H.J. Lewandowski, D.M. Harber, D.L. Whitaker, and E.A. Cornell, Phys. Rev. Lett. **88**, 070403 (2002).

[10] N.F. Ramsey, *Molecular Beams* (Clarendon Press, Oxford, 1956).

[11] J.M. McGuirk, H.J. Lewandowski, D.M. Harber, T. Nikuni, J.E. Williams, and E.A. Cornell, Phys. Rev. Lett. **89**, 090402 (2002).

[12] At $n = 10^{13}$ cm^{-3} $\nu_{\text{spin wave}} = 5$ Hz, so interrogation times of 20 ms are acceptable.

[13] Where $\beta = 431.359\,57(9)$ Hz/G^2 and $\nu_{min} = 6\,834\,678\,113.59(2)$ Hz [9].

[14] M.Ö. Oktel, T.C. Killian, D. Kleppner, and L.S. Levitov, Phys. Rev. A **65**, 033617 (2002).

[15] M.Ö. Oktel and L.S. Levitov, Phys. Rev. A **65**, 063604 (2002).

[16] J.E. Williams, T. Nikuni, and C.W. Clark, Phys. Rev. Lett. **88**, 230405 (2002).

[17] E.G.M. van Kempen, S.J.J.M.F. Kokkelmans, D.J. Heinzen, and B.J. Verhaar, Phys. Rev. Lett. **88**, 093201 (2002).

[18] The Thomas-Fermi radius (and to a lesser extent the critical temperature) are of course interaction dependent, and therefore using measurements of these quantities to calibrate densities in order to characterize interaction strengths is somewhat circular. Our directly measured value of $\alpha_{ii}^{nc}/\alpha_{ii}^{c} = 2.1(2)$, on the other hand, is based predominantly on measured spatial extent of the cloud and on an absolute determination of the absorption depth, and therefore it is only weakly model dependent. We quote the "worst-case corrected value" of $\alpha_{ii}^{nc}/\alpha_{ii}^{c} = 1.7(2)$ in order to put a reasonable limit on the size of possible systematic errors, and not because we feel it is the preferred value.

[19] D.S. Hall, M.R. Matthews, J.R. Ensher, C.E. Wieman, and E.A. Cornell, Phys. Rev. Lett. **81**, 1539 (1998).

[20] When we changed the length of the first Ramsey pulse, the second pulse length was also changed such that the two pulses combined to form a π pulse, which gives us the maximum signal to noise.

[21] The quoted chirp limit of $-0.2(3)$ Hz includes a correction to account for a small frequency change associated with decay of total atom number during the measurement time. For each data set the number decay was found by allowing an exponential decay in the fit of the Ramsey fringes (not to be confused with the decay in Ramsey fringe contrast associated with decoherence), resulting in a correction amounting to -0.74 Hz on average.

[22] Fitting the decay of the integrated transverse magnetization to $e^{-(t/\tau)^2}$, the same functional form as we fit to the actual experimental data, gives values typically within 5%, and at worst 12%, of the $1/e$ time.

[23] W.M. Itano, J.C. Bergquist, J.J. Bollinger, J.M. Gilligan, D.J. Heinzen, F.L. Moore, M.G. Raizen, and D.J. Wineland, Phys. Rev. A **47**, 3554 (1993).